Mon. Not. R. Astron. Soc. **000**, 1–?? (...) Printed 11 March 2009 (MN LATEX style file v2.2)

The bulk kinetic power of radio jets in active galactic nuclei

Minfeng Gu [1⋆], Xinwu Cao[1], D. R. Jiang[1]
[1] *Key Laboratory for Research in Galaxies and Cosmology, Shanghai Astronomical Observatory, Chinese Academy of Sciences, 80 Nandan Road, Shanghai 200030, China*

11 March 2009

ABSTRACT

Based on the Königl's inhomogeneous jet model, we estimate the jet parameters, such as bulk Lorentz factor Γ, viewing angle θ and electron number density $n_{\rm e}$ from radio VLBI and X-ray data for a sample of active galactic nuclei (AGNs) assuming that the X-rays are from the jet rather than the intracluster gas. The bulk kinetic power of jets is then calculated using the derived jet parameters. We find a strong correlation between the total luminosity of broad emission lines and the bulk kinetic power of the jets. This result supports the scenario that the accretion process are tightly linked with the radio jets, though how the disk and jet are coupled is not revealed by present correlation analysis. Moreover, we find a significant correlation between the bulk kinetic power and radio extended luminosity. This implies that the emission from the radio lobes are closely related with the energy flux transported through jets from the central part of AGNs.

Key words: galaxies: active – galaxies: jets – quasars: emission lines

1 INTRODUCTION

The formation of highly relativistic jets in active galactic nuclei (AGNs) is one of the unsolved fundamental problems in astrophysics (e.g. Meier et al. 2001). It has been assumed that jets are produced close to the central black hole, involving power extraction from the black hole spin (Blandford & Znajek 1977; Macdonald & Thorne 1982; Thorne & Blandford 1982) and/or from the accretion disk (Blandford & Payne 1982). Although the jet formation remains unclear, the estimate of the jet power is of fundamental physical interest, since it can be used to quantify the power emerging from the central engine of the radio source. Recently, the prescriptions for AGN feedback have been introduced into semi-analytic models of galaxy formation, and both Bower et al. (2006) and Croton et al. (2006) show that this feedback is able to solve the issue of the bright end of the luminosity function, whilst simultaneously solving other problems of galaxy formation models such as why the most massive galaxies are so red. Although the form of the AGN feedback adopted is very different in the two prescriptions, the relativistic ejecta from the AGN is a conceivably important ingredient of AGN feedback. Indeed, in clusters of galaxies containing powerful radio sources, X-ray observations have revealed bubbles and cavities in the hot intracluster medium, evacuated by the expanding radio source (e.g. McNamara et al. 2000; Fabian et al. 2003). Recent studies showed that the mechanical luminosity of radio sources are sufficient to suppress cluster cooling flows (Best et al. 2006; Nusser, Silk & Babul 2006). To understand the interaction between the radio sources and the surrounding medium, it is clearly important to estimate the bulk kinetic power of radio jets, since the expanding radio sources provides a direct way for the AGN output to be coupled to its environment.

The relation between the jets and the accretion processes in active galactic nuclei has been extensively explored by many authors and in different ways. The strong correlations have been found between the low-frequency radio and narrow-line luminosities of 3C radio sources (Baum & Heckman 1989; Rawlings et al. 1989; Saunders et al. 1989), and also between the broad line and extended radio luminosity for radio-loud quasars (e.g. Cao & Jiang 2001). The link between the jets and the accretion processes can also been studied through exploring the relationship between luminosity in line emission and

⋆ E-mail: gumf@shao.ac.cn

kinetic power of jets in different scales (Rawlings & Saunders 1991; Celotti & Fabian 1993; Falcke, Malkan & Biermann 1995; Wang, Luo & Ho 2004). Rawlings & Saunders (1991) used the narrow-line luminosity as indicative of the accretion power and estimated the power transported by the jet from the energy content and lifetime of the radio lobes, finding a good correlation between the two. Using radio data on very long-baseline interferometry (VLBI) scales and the standard synchrotron self-Compton (SSC) theory, Celotti & Fabian (1993) estimated the jet kinetic power to put constraints on the matter content of jets. It offers some clues to understand the fundamental questions of the mechanisms, such as the collimation and acceleration of jets. Celotti, Padovani & Ghisellini (1997, hereafter C97) explored the relation of luminosity in broad emission lines with the kinetic power of the jets for a sample of radio-loud AGNs. Their estimate of the bulk kinetic power is based on the adoption of the SSC model applied to the radio VLBI data and X-ray (or optical) fluxes. Lacking more accurate information, the minimum Γ for any given δ [i.e. $\Gamma = 0.5(\delta + 1/\delta)$] is used in the derivation of bulk kinetic power for objects with $\delta > 1$, otherwise the Γ is derived from an average δ. They found a suggestive hint of correlation between these two luminosities which is in favour of a link between the accretion process and the jets. However, by re-estimating the luminosity in broad emission lines on the sample of C97, Wang et al. (2004) argued that the jet bulk kinetic power is significantly correlated with the disk luminosity. Maraschi & Tavecchio (2003, hereafter MT03) found that the jet power is linearly proportional to the disk power for a sample of blazars, for which the jet powers were estimated using physical parameters determined from uniformly modeling their spectral energy distributions. However, by studying a sample of quasars from Wang et al. (2004), Punsly & Tingay (2005) argued that the bulk kinetic power and the bolometric luminosity are very weakly correlated in radio-loud quasars that possess blazar cores.

In the framework of the relativistic beaming and the SSC model, the physical quantities in the jets can be estimated using the VLBI observations and the X-ray flux density. Marscher (1987) derived the beaming parameters on the assumption of homogeneous spherical emission plasma. Ghisellini et al. (1993) adopted Marscher's approach and obtained the Doppler boosting factor δ for 105 sources. Moreover, Readhead (1994) estimated the equipartition Doppler boosting factor $\delta_{\rm eq}$, assuming that the sources are in equipartition between the energy of radiating particles and the magnetic field. Güijosa and Daly (1996) derived the $\delta_{\rm eq}$ for the same sample in Ghisellini et al. (1993). The variability Doppler factor $\delta_{\rm var}$ is derived on the assumption that the associated variability brightness temperature of total radio flux density flares are caused by the relativistic jets (Lähteenmäki & Valtaoja 1999). The advantage of homogeneous sphere model is that the formalism is simple and the value of δ derived is independent on the cosmology model. However, it is generally difficult to know the component angular size and the flux at the turnover frequency, so one has to assume that the VLBI observing frequency is the synchrotron self-absorption frequency. In addition, the dependence of core size on the observing frequency in some sources is inconsistent with the homogeneous spherical assumption. Blandford and Königl (1979) and Königl (1981) presented an inhomogeneous relativistic jet model, in which both the flat spectrum characteristics of some AGNs and the dependence of the core size on the observing frequency could be well explained. Based on their model, a new approach has been proposed to derive the jet parameters including bulk Lorentz factor Γ, viewing angle θ and electron number density $n_{\rm e}$ in the jets (Jiang, Cao & Hong 1998, hereafter J98). The proper motion measurements on the jets' components were adopted in their calculations. The correlation between the brightness temperature in the source rest frame and the derived Doppler factor suggested that the derived values of beaming parameters are quite reliable (J98). Moreover, the derived beaming parameters from the homogeneous sphere model is in general consistent with that from their inhomogeneous jet model.

In this work, we follow the method of J98 to derive the physical quantities of jets for a large sample of AGNs, then re-analyze the relation between the luminosity in broad line emissions and the bulk kinetic power of the jets. In Section 2, we describe the sample of sources. The method of jet parameters derivation and the estimate of jet kinetic power are outlined in Section 3. Section 4 includes the results and discussion. In the last section, we draw our conclusions. The cosmology with $H_0 = 70$ km s^{-1} Mpc^{-1}, $\Omega_{\rm M} = 0.3$, and $\Omega_\Lambda = 0.7$ have been adopted throughout the paper.

2 THE SAMPLE

In order to use inhomogeneous jet model to estimate the jet parameters, all sources should have VLBI measurements of proper motion of outflowing plasma. Combining with the relevant data of sources, such as the radio flux density, the size of the core and X-ray flux density, the jet parameters can be derived (J98). After searching the literature, our sample is constructed, which consists of 128 sources, including 94 quasars, 26 BL Lac objects and 8 radio galaxies. The observational data for the sample are presented in Table 1: (1) IAU name; (2) classification of the source (Q= quasars; Qc= core-dominated quasars; Ql= lobe-dominated quasars; Qp= GHz peaked quasars; BL= BL Lac objects; G= radio galaxies); (3) redshift z; (4) observation frequency $\nu_{\rm s}$ in GHz; (5) core radio flux density $f_{\rm c}$ at frequency $\nu_{\rm s}$; (6) VLBI core size $\theta_{\rm d}$ in mas; (7) reference for the VLBI data; (8) the proper motion $\mu_{\rm app}$; (9) reference for the proper motion; (10) 1 keV X-ray flux density $f_{\rm 1keV}$ in μJy; (11) reference for the X-ray flux.

When there are more than one moving components, we adopted the fastest one, which is regarded as a good approximation of jet bulk motion. In addition, we use the core flux density measured at the highest frequency, when VLBI core was measured

at more than one frequency. We assume that all the observed X-ray flux density is attributable to the SSC emission in the derivation, which will introduce some uncertainties. However, the derived jet parameters are not sensitive to the adopted X-ray flux density (J98). The redshift of 0716+714 is not available, and a value of 0.3 is assumed in the calculation. To calculate the total luminosity of broad emission lines, the available measurements of various broad emission lines for each source are collected from literatures. Moreover, we search the literatures and collect all available radio extended emission data from VLA observations for each source. The data are available for all 128 sources, of which the data from Australia Telescope Compact Array (ATCA) are used for the southern source 0208-512, and only upper limit is available for 8 sources due to the faintness or non-detection of extended emission. The extended flux density is k-corrected to 5 GHz in the rest frame of the source assuming $\alpha_{\rm e} = -1$ ($f_{\rm ext} \propto \nu^{\alpha_{\rm e}}$).

3 BULK KINETIC POWER

We estimate the bulk kinetic power based on the inhomogeneous jet model (Königl 1981). Using VLBI radio data, including proper motion of plasma, and X-ray fluxes, we can calculate the comoving electron number density $n_{\rm e}$, the magnetic field intensity, Lorentz factor Γ and the viewing angle θ. A brief description of the method is given below, and we refer to J98 and references therein for a complete description. In brief, the jet parameters were calculated by relating the model predicted size of optically think region in the jet, radio emission from the optically think region along the jet, SSC X-ray emission from the unresolved jet, and the apparent transverse velocity to the observables of radio core size, radio core flux density, X-ray flux density, and the proper motion. In this paper, we assume that the X-rays are from the jet rather than the intracluster gas and the radio blob speed is the jet flow speed.

In Königl's inhomogeneous jet model, the magnetic field $B(r)$ and the number density of the relativistic electrons $n_{\rm e}(r,\gamma_{\rm e})$ in the jet are assumed to vary with the distance from the apex of the jet r as $B(r) = B_1(r/r_1)^{-m}$ and $n_{\rm e}(r,\gamma_{\rm e}) = n_1(r/r_1)^{-n}{\gamma_{\rm e}}^{-(2\alpha+1)}$, respectively, where $r_1 = 1$ pc and $\gamma_{\rm e}$ is the Lorentz factor of the electron in the jet. Given that the bulk motion velocity of the jet is βc (corresponding to a Lorentz factor Γ) with an opening half-angle ϕ, and the axis of the jet makes an angle θ with the direction of the observer, the distance from the origin of the jet, $r(\tau_{\nu_{\rm s}} = 1)$, at which the optical depth to the synchrotron self-absorption at the observing frequency $\nu_{\rm s}$ equals unity, is given as

$$\frac{r(\tau_{\nu_{\rm s}}=1)}{r_1} = (2c_2(\alpha)r_1 n_1 \phi \csc\theta)^{2/(2\alpha+5)k_{\rm m}} (B_1\delta)^{(2\alpha+3)/(2\alpha+5)k_{\rm m}} (\nu_{\rm s}(1+z))^{-1/k_{\rm m}} \quad (1)$$

where $c_2(\alpha)$ is the constant in the synchrotron absorption coefficient, δ is the Doppler factor, and $k_{\rm m} = [2n + m(2\alpha+3) - 2]/(2\alpha+5)$.

The projection of the optically thick region in the jet is then used as the observed VLBI core angular size $\theta_{\rm d}$,

$$\theta_{\rm d} = \frac{r(\tau_{\nu_{\rm s}}=1)\sin\theta}{D_{\rm a}} \quad (2)$$

where $D_{\rm a}$ is the angular diameter distance of the source.

By integrating the emission from the optically thick region along the jet, the radio flux of the core can be obtained

$$s(\nu_{\rm s}) = \frac{r_1^2\phi\sin\theta}{(4+m)\pi D_{\rm a}^2}\frac{c_1(\alpha)}{c_2(\alpha)} B_1^{-1/2}\nu_{\rm s}^{5/2}\left(\frac{\delta}{1+z}\right)^{1/2}\left(\frac{r(\tau_{\nu_{\rm s}}=1)}{r_1}\right)^{(4+m)/2} \quad (3)$$

where $\nu_{\rm s}$ is the VLBI observing frequency, and $c_1(\alpha)$ and $c_2(\alpha)$ are the constants in the synchrotron emission and absorption coefficients, respectively.

Equation (13) in Königl's work gives the X-ray flux density estimation from an unresolved jet. As in J98, we adopt the expression in the frequency region $\nu_{\rm c} > \nu_{\rm cb}(r_{\rm M})$, where $r_{\rm M}$ is the smallest radius from which optically thin synchrotron emission with spectral index α is observed (Königl 1981).

The proper motion observed with VLBI can be converted to the apparent transverse velocity $\beta_{\rm app}$, which is related to the bulk velocity of the jet βc and viewing angle θ,

$$\beta_{\rm app} = \frac{\beta\sin\theta}{1-\beta\cos\theta} \quad (4)$$

Given the three parameters α, m, n, and the relation between the opening half angle ϕ and the Lorentz factor Γ, the parameters of an inhomogeneous jet can be derived from VLBI and X-ray observations, using the above equations and equation (13) in Königl (1981). In our calculation, we take $\alpha = 0.75$, the opening half-angle $\phi = 1/\Gamma$, and assume $m = 1$, $n = 2$ corresponding to a free jet (Hutter & Mufson 1986).

With the estimated comoving total electron number density $n_{\rm t}$, Lorentz factor Γ and the cross section of the jet S, the bulk kinetic power is then derived as

$$L_{\rm kin} = Sn_{\rm t}(m_{\rm e}\langle\gamma\rangle + m_+\langle\gamma_+\rangle)c^2\Gamma(\Gamma-1)\beta c, \quad (5)$$

where $m_{\rm e}$ is the electron rest mass, m_+ is the rest mass of positive charge, $\langle\gamma\rangle$ is the average Lorentz factor of electrons, and $\langle\gamma_+\rangle$ is the average Lorentz factor of positive charges. For a conical jet with an opening half-angle ϕ, $S = 2\pi r^2(1-\cos\phi)$. The total electron number density $n_{\rm t}$ is given by

$$n_{\rm t} = \int_{\gamma_{\rm min}}^{\gamma_{\rm max}} n_{\rm e}(r,\gamma_{\rm e})d\gamma_{\rm e}, \tag{6}$$

The bulk kinetic power of the inhomogeneous jet becomes

$$L_{\rm kin} = \alpha^{-1}\pi r^{2-n} r_1^n n_1 \gamma_{\rm min}^{-2\alpha}(1-\cos\phi)(m_{\rm e}\langle\gamma\rangle + m_+\langle\gamma_+\rangle)\Gamma(\Gamma-1)\beta c^3 \tag{7}$$

With our adoption of $\alpha = 0.75$, $\phi = 1/\Gamma$, $m = 1$, and $n = 2$, the bulk kinetic power of the jet is then given by

$$L_{\rm kin} = \frac{4}{3}\pi r_1^2 n_1 \gamma_{\rm min}^{-\frac{3}{2}}(1-\cos 1/\Gamma)(m_{\rm e}\langle\gamma\rangle + m_+\langle\gamma_+\rangle)\Gamma(\Gamma-1)\beta c^3 \tag{8}$$

We note that the bulk kinetic power $L_{\rm kin}$ is independent of r, since $n = 2$ is adopted in the calculation and the particle conservation is then satisfied along r. $L_{\rm kin}$ is largely dependent of the matter content of jets and the low energy cut-off $\gamma_{\rm min}$ of electrons. In present, the jet composition is still unclear, i.e. whether electron-positron or electron-proton (see Worrall & Birkinshaw 2006, for a recent review and reference therein). However, for an electron-proton plasma, $\gamma_{\rm min} \sim 100$ has been suggested, while $\gamma_{\rm min}$ could be as low as unity for an electron-positron jet (e.g. Celotti & Fabian 1993). The detection of circular polarization strongly suggests that the jets are electron-positron plasmas with $\gamma_{\rm min} \lesssim 10$ at least in some sources (e.g. Wardle et al. 1998). The similar conclusion is also arrived from powerful large scale X-ray jets, if they are interpreted as inverse-Compton scattering of cosmological microwave background photons in fast jets. From equation (8), however, we find that the bulk kinetic power $L_{\rm kin}$ for a electron-proton jet with $\gamma_{\rm min} \sim 100$ ($m_+ = 1836\ m_{\rm e}$ and $\langle\gamma_+\rangle = 1$) is in agreement with that of electron-positron one with $\gamma_{\rm min} \lesssim 10$ ($m_+ = m_{\rm e}$ and $\langle\gamma_+\rangle = \langle\gamma\rangle$) within a factor of three. In present work, we calculate the bulk kinetic power $L_{\rm kin}$ assuming electron-positron jets with $\gamma_{\rm min} = 1$. A change to $\gamma_{\rm min} = 10$ will uniformly reduce $L_{\rm kin}$ by about a factor of three. However, in this work, we mainly focus on the correlation between the bulk kinetic power $L_{\rm kin}$ and the luminosity in broad emission lines $L_{\rm BLR}$, therefore, the value of $\gamma_{\rm min}$ will not affect the correlation analysis, if the assumption that all sources have the same value $\gamma_{\rm min}$ holds.

The observational data necessary for calculations are presented in Table 1. Following C97, we use the line ratios reported by Francis et al. (1991) and add the contribution from line $\rm H_\alpha$ to derive the total broad line luminosity $L_{\rm BLR}$. The derived values of jet parameters, $L_{\rm kin}$, $L_{\rm BLR}$ and 5 GHz radio extended luminosity for our sources are listed in Table 2: (1) IAU name; (2) the viewing angle of jet θ; (3) the Lorentz factor Γ; (4) the Doppler factor δ; (5) the normalization factor of electron energy distribution n_1; (6) the bulk kinetic power of jet $L_{\rm kin}$; (7) the total luminosity in broad emission lines $L_{\rm BLR}$; (8) the references for flux of broad emission lines used to estimate $L_{\rm BLR}$; (9) the radio extended 5 GHz luminosity $L_{\rm ext,5GHz}$; (10) the references for the radio extended flux.

4 RESULTS AND DISCUSSION

4.1 Bulk kinetic power and BLR luminosity

Out of 128 sources, the measurements of various broad emission lines are only available for 98 sources from literature or Sloan Digital Sky Survey (SDSS) spectra, including 81 quasars, 15 BL Lac objects, and 2 radio galaxies. The reason of no measurements for remaining 30 sources could be either the non-detection of broad emission lines in 11 BL Lac objects and 6 radio galaxies, or no published line flux measurements for 13 quasars. We have calculated the total luminosity of broad emission lines for these 98 sources. The relationship between $L_{\rm BLR}$ and $L_{\rm kin}$ is shown in Fig. 1. We find a strong correlation between these two luminosities with a Spearman correlation coefficient of $r = 0.565$ at $\gg 99.99\%$ confidence. It should be noted that this correlation may be caused by the common dependence on redshift. We present the bulk kinetic power and BLR luminosity as functions of redshift z for the sample in Fig. 2. We therefore use the partial Spearman rank correlation method (Macklin 1982) to check this correlation. Still, a significant correlation with a correlation coefficient of 0.323 is present at about 99.9% significance level between $L_{\rm BLR}$ and $L_{\rm kin}$, independent of the redshift. We also perform a statistic analysis on the sources in the restricted redshift range $0.5 < z < 1.0$. For this subsample of sources, we check the correlation between luminosity and redshift, and no correlation between either the bulk kinetic power or the BLR luminosity and redshift, is found (see Fig. 2), while a significant correlation is still present at 99.1 per cent confidence between the bulk kinetic power and total broad-line luminosity (see Fig. 1). Therefore, we conclude that this correlation might be intrinsic, at least for our present sample. Assuming that the BLR luminosity is due to the reprocessing of the ionizing radiation from the accretion disk, it therefore strongly supports the scenario of a tight connection between the relativistic jet and the accretion process.

For all 98 sources, the ordinary least-squares (OLS) bisector method gives the following fit in Fig. 1:

$$\log\ L_{\rm kin} = (0.86 \pm 0.07)\ \log\ L_{\rm BLR} + (8.78 \pm 3.05) \quad (9)$$

Apart from finding a significant correlation, Rawlings & Saunders (1991) found that the relationship between the bulk kinetic power and narrow line luminosity is close to proportionality, $Q \propto L_{\rm NLR}^{0.9\pm0.2}$, which extends over four orders of magnitude. Our relation of $L_{\rm kin} \propto L_{\rm BLR}^{0.86\pm0.07}$ is consistent with the relationship between the jet power and narrow-line luminosity in Rawlings & Saunders (1991) and Celotti & Fabian (1993), whereas it is somehow deviated, but not much, from the linear relation between the jet power and disk power found by MT03. However, it is much steeper than that of Wang et al. (2004), $L_{\rm kin} \propto L_{\rm BLR}^{0.37}$. Although what cause these differences is unclear, we note that the methods used to estimate the jet power in MT03 and Wang et al. (2004) are different from ours. The jet powers of MT03 were estimated using physical parameters determined from uniformly modeling their spectral energy distributions, while Wang et al. (2004) directly used the jet bulk kinetic power from C97, which was estimated using the homogeneous sphere SSC model. Moreover, MT03 obtained their disk luminosities either directly from the optical-UV luminosity of the big blue bump or from the original prescription of C97. The method Wang et al. used to estimate $L_{\rm BLR}$ is basically same as ours. In addition, Wang et al. sample consists of 35 blazars, and only 16 sources (11 quasars and 5 BL Lac objects) were considered in MT03. Their samples are much smaller than our sample. Whether these factors influence the dependence of $L_{\rm kin}$ on $L_{\rm BLR}$ needs further investigations. Despite this, our results strongly support the scenario that the accretion process are tightly linked with the kinetic power in the jet, though how the disk and jet are coupled is not revealed by present correlation analysis.

In general, BL Lac objects, which is thought to be FR I radio galaxies pointing at us, are characterized by very weak or absent emission lines, invisible blue bumps, and relatively powerful jets. From Fig. 1, it is clear that BL Lac objects have fainter broad-line luminosity compared to quasars, though only 15 BL Lac objects are in our sample. We find that the $L_{\rm kin} - L_{\rm BLR}$ relation of BL Lac objects deviate from that of quasars, although it generally follows that of the whole sample. The linear fit using OLS bisector method for BL Lac objects shows

$$\log\ L_{\rm kin} = (0.71 \pm 0.12)\ \log\ L_{\rm BLR} + (15.85 \pm 4.99) \quad (10)$$

while for quasars, we have

$$\log\ L_{\rm kin} = (1.12 \pm 0.08)\ \log\ L_{\rm BLR} - (2.94 \pm 3.39) \quad (11)$$

Although the mechanism of jet formation is unclear, the different dependence of $L_{\rm kin}$ on $L_{\rm BLR}$ in BL Lac objects and quasars can be due to the difference of the accretion power as measured in units of the Eddington one. Compared to quasars, BL Lac objects are characterized by radiatively inefficient accretion disks (Cao 2003), thus in these sources the jet power may be relatively dominant. To further check the $L_{\rm kin} - L_{\rm BLR}$ correlation in Fig. 1, we re-examine it for quasars only. When BL Lac objects and radio galaxies are excluded, we still find a strong correlation between $L_{\rm BLR}$ and $L_{\rm kin}$ with correlation coefficient of $r = 0.380$ at 99.95% confidence. This further confirms the tight link between the accretion process and the kinetic power in the jet.

If the accretion process and the jet formation are indeed closely related, then the tight relation between the mass channelled into jets and that accreted by black hole would be expected. We then investigate the relationship between the mass outflowing rate and accretion one, on assumption of $L_{\rm bol} \approx 10 L_{\rm BLR}$ (Netzer 1990), and with the expression of the kinetic and the accretion powers as

$$L_{\rm kin} = \Gamma \dot{M}_{\rm out} c^2;\ L_{\rm bol} = \eta \dot{M}_{\rm in} c^2, \quad (12)$$

where $\dot{M}_{\rm out}$ is the mass outflowing rate, Γ is jet Lorentz factor, $\dot{M}_{\rm in}$ is the mass accretion rate, and η is the efficiency of mass to energy conversion for accretion. Adopting the typical value of $\eta \sim 0.1$, we find a significant correlation between $\dot{M}_{\rm out}$ and $\dot{M}_{\rm in}$ for whole sample, with a Spearman correlation coefficient 0.514 at $\gg 99.99\%$ confidence. This implies that the mass outflowing rate in jet is closely linked with the accretion one in accretion disk.

The present analysis is based on the derivation of jet parameters using inhomogeneous jet model. Some parameters and assumptions are adopted in the inhomogeneous jet model to derive the physical quantities of the jet (J98), which may induce some uncertainties in the estimation of $L_{\rm kin}$. The most important is probably the intrinsic differences of the low energy cut-off $\gamma_{\rm min}$ of electrons between the radio sources themselves. In this work, we adopt the same value of $\gamma_{\rm min}$ in deriving the kinetic power of the jet, which may not be true. However, we are not able to estimate $\gamma_{\rm min}$ for each source at present stage. Nevertheless, we believe that the adoption of an uniform $\gamma_{\rm min}$ for all sources in the correlation analysis would not affect the main conclusion drawn here. Moreover, our results are based on the assumption of $\alpha = 0.75$, $m = 1$, and $n = 2$, and we adopted these same values for all sources in our model calculation. However, we find that the alternative adoption of α, m, and n do not change our main conclusion, e.g. the strong correlation between $L_{\rm kin}$ and $L_{\rm BLR}$. In practice, the sources may have different values of parameters α, m, and n, and, in principle, these parameters could be constrained by the observable quantities (J98). Unfortunately, the information is only found for a few cases through multi-frequencies VLBI observations. Further high resolution multi-frequencies VLBI observations would be helpful to improve our model calculations.

It should be noted that not all sources in our sample have available BLR luminosity. Therefore, the selection effects may be introduced in our correlation analysis, i.e. those sources without published broad line flux measurements may likely be

biased towards those with weak lines, especially the 11 BL Lac objects without broad line flux measurements. To evaluate the selection effects, we tentatively calculate the upper limit of BLR luminosity assuming equivalent width of broad Hβ line EW < 5Å for these 11 BL Lacs. Moreover, we calculate the BLR luminosity for 13 quasar without BLR luminosity by randomly assigning the BLR flux in the BLR flux range of 81 quasars with BLR luminosity. Combining these 24 sources with those having BLR luminosity, we use the Astronomy Survival Analysis (ASURV) package (Isobe, Feigelson & Nelson 1986) to investigate the correlation by taking the upper limit into account. A significant correlation is still found with Spearman's rho correlation method. This correlation is confirmed by using the partial correlation method for censored data of Akritas & Siebert (1996) to exclude the common dependence of redshift. Furthermore, the correlation remains significant even we conservatively adopt broad Hβ line EW < 1Å for 11 BL Lacs. It thus seems that the non-BLR luminosity sources do not affect our correlation results.

4.2 Bulk kinetic power and radio extended luminosity

In Fig. 3, the relation between bulk kinetic power and 5 GHz radio extended luminosity is shown for all 128 sources. Since only the upper limit of 5 GHz extended luminosity is given for 8 sources, we use ASURV package (Isobe et al. 1986) to investigate the correlation and perform the linear regression analysis for our censored data. We find the significant correlation with a Spearman's rho correlation coefficient of $r = 0.493$ at $\gg 99.99\%$ confidence. Using the partial correlation method for censored data of Akritas & Siebert (1996) to exclude the common dependence of redshift, a significant correlation is still present between $L_{\rm ext,5GHz}$ and $L_{\rm kin}$. We use the Schmitt-binning method (Schmitt 1985) to perform y/x and x/y fits and then calculate a bisector of these two fits, as described in Shapley, Fabbiano & Eskridge (2001) (see also Isobe et al. 1990). We obtain:

$$\log\ L_{\rm kin} = (0.82 \pm 0.09)\ \log\ L_{\rm ext,5GHz} + (12.38 \pm 4.00) \tag{13}$$

which is shown as the solid line in Fig. 3.

The extended radio flux is usually emerged from the optically thin radio lobes, and thus is free from the Doppler boosting effects, since the lobe material is generally thought to be of low enough bulk velocity. Therefore, the extended radio luminosity can be a good tracer of jet power (e.g. Cao & Jiang 2001). The significant correlation between $L_{\rm kin}$ and $L_{\rm ext,5GHz}$ implies that the emission from radio lobes are tightly related with the energy ejected into the jet from the central parts of AGNs. This result is not surprising, as it could be naturally expected. Although the detailed mechanism of jet formation is still unclear, the energy can be transported through the jets to the radio lobes once the jets are generated. Most of the energy flux of jets is not radiated away, instead are in mechanical form (i.e. bulk kinetic power), of which the particles and fields are necessary to produce the synchrotron luminosity that is detected in the radio lobes. If the radiative efficiency of radio lobes are similar between our radio sources, then the tight link between the bulk kinetic power of jets and the radio extended emission is expected, since the latter is optically thin and not effected from the Doppler enhancement.

Motivated largely by the observed effects of radio-loud AGN on their environments at galaxy cluster scales (e.g. Fabian et al. 2003), whether the heating effect of AGN activity, particularly radio-loud AGN activity, can balance the cooling of the gas has recently arose much interest (e.g. Best et al. 2005, 2006; Croton et al. 2006; Nusser, Silk & Babul 2006). Independently of the radio properties, Bîrzan et al. (2004) estimated the mechanical luminosity associated with the radio source, by studying the cavities and bubbles that are produced in clusters and groups of galaxies due to the interactions between the radio sources and the surrounding hot gas. The dependence of the mechanical luminosity on the 1.4 GHz radio luminosity of the associated radio sources, $L_{\rm mech} \propto L_{\rm radio}^{0.44\pm0.06}$ fitted for their entire sample, is somewhat deviated from ours (equation 13). However, the dependence for the radio-filled cavities only (see Bîrzan et al. 2004 for details), $L_{\rm mech} \propto L_{\rm radio}^{0.6\pm0.1}$ is marginally consistent with ours within the errors. Despite this, we note that their work is mainly based on the galaxy clusters and the radio sources in these clusters, however, our present study focused on the powerful radio sources. Moreover, the jet power is estimated using different methods, and the different radio luminosity is used. In present, we are not able to draw a solid calibration between the radio emission and the kinetic power of jets, and it needs further investigations.

Despite the strong correlation presented in Fig. 3, the significant scatter is clearly seen. This is not surprising since even for a source of fixed jet kinetic power the radio luminosity changes as the source ages (e.g. Kaiser et al. 1997). However, there are several factors that can introduce the scatter into the correlation. We note that the observed radio extended emission has been dissipated over a long period, which is not contemporaneous with the estimated bulk kinetic power. Moreover, when jets transported the energy flux from the central parts of AGNs to outer radio lobes, the jets can be decelerated by the interaction with the nuclear ISM and/or the entrainment of external gas (e.g. Tavecchio et al. 2006). As a result, the part of jet power will be lost to the ISM. In some extreme cases, the kinetic power of the jet on kiloparsec scales could be about three orders of magnitude weaker than the power of the jet on 10 - 100 pc scales due to the jet-ISM interaction, i.e. virtually all of the jet power can be lost to the ISM within the inner kiloparsec (Gallimore et al. 2006). Consequently, the difference of jet-ISM interactions between the radio themselves may bring scatter. Furthermore, part of the scatter may be due to the different radiative efficiency in individual source.

4.3 Bulk kinetic power versus radiative luminosity

It is well known that the monochromatic radio luminosity does not provide a good indicator of the mechanical energy output of a radio source. Radio sources are inefficient radiators. Bicknell (1995) estimated that the kinetic energy output of a radio jet is typically a factor of 100-1000 higher than the total radio luminosity of a radio source, which is recently confirmed by the observations of Bîrzan et al. (2004).

We estimate the amount of radiative dissipation on parsec scales, i.e. the ratio of $L_{\rm kin}/L_{\rm rad,in}$ of the bulk kinetic power to the intrinsic radiative luminosity. The latter has been computed from the observed VLBI radio core fluxes. The Doppler correction on the monochromatic luminosity is assumed to be $L_{\rm obs} = \delta^p\ L_{\rm int}$, where $L_{\rm obs}$ and $L_{\rm int}$ are the observed and intrinsic (comoving) luminosities. We can calculate p from the dependence of the core radio flux on the Doppler factor from equation (3), in which p is dependent of the value of α, m and n. In Fig. 4, we show the histogram of the derived ratios $L_{\rm kin}/L_{\rm rad,in}$. We find that the ratio covers about three orders of magnitude with the average value $< \log\ (L_{\rm kin}/L_{\rm rad,in}) >= 4.98 \pm 0.79$. This result is consistent with that of Celotti & Fabian (1993), although a wider spread of ratio distribution in their sources. The results indicate that for all sources the kinetic power is dominant with respect to the radiative output, and consequently that the radiative dissipation is not an efficient process. Moreover, the large variation in this ratio indicates that the radio luminosity is not necessarily a reliable probe of the available bulk kinetic power.

It is commonly accepted that the synchrotron emission of blazars can extend to optical and even X-ray region, which can dominate over the thermal emission from accretion disk, and the radio emission as well. The spectral energy distribution (SED) of blazars is usually composed of two peaks, of which the first one is dedicated to the synchrotron emission for jets, and the second is due to the inverse Compton process (Fossati et al. 1998; Ghisellini et al. 1998). Thus the total radiative luminosity of the jets, if we can estimate from integrating over the synchrotron domain of SED, can represent the minimum power that must be associated with the jet in order to produce the observed luminosity. In this sense, the radio emission solely might not be a good indicator of the radiative output from the radio jets, i.e. the radiation losses of the kinematic jet flow. MT03 found that the radiative efficiency, i.e. the ratio of the total radiative luminosity of the jet to the jet power, can be in the range 1%-10%. Even so, the radiative dissipation is still not an efficient process, and the most of the energy flux is in the kinetic form. In present, it is not readily to estimate the total radiative luminosity of jets for our sample. Nevertheless, we believe that the inefficient radiators of radio sources would be still retained.

5 CONCLUSIONS

Based on the inhomogeneous jet model, we have calculated the jet parameters for a sample of AGNs. The bulk kinetic power of radio jets are then estimated using the derived jet parameters. We found a significant correlation between the bulk kinetic power of the relativistic jet and the total luminosity in broad emission lines, implying a tight link between the jet and accretion process. Moreover, the bulk kinetic power of jets are strongly correlated with the radio extended luminosity. This indicates a closely connection between the emission from radio lobes and the energy flux transported through jets from the central parts of AGNs. In addition, we found that the bulk kinetic power is dominant with respect to the radiative output, which means the radiative dissipation is not an efficient process.

ACKNOWLEDGMENTS

We thank the anonymous referee for insightful comments and constructive suggestions. This work is supported by National Science Foundation of China (grants 10633010, 10703009, 10833002, 10773020 and 10821302), 973 Program (No. 2009CB824800), and the CAS (KJCX2-YW-T03). This research has made use of the NASA/ IPAC Extragalactic Database (NED), which is operated by the Jet Propulsion Laboratory, California Institute of Technology, under contract with the National Aeronautics and Space Administration.

Funding for the SDSS and SDSS-II has been provided by the Alfred P. Sloan Foundation, the Participating Institutions, the National Science Foundation, the U.S. Department of Energy, the National Aeronautics and Space Administration, the Japanese Monbukagakusho, the Max Planck Society, and the Higher Education Funding Council for England. The SDSS Web Site is http://www.sdss.org/.

The SDSS is managed by the Astrophysical Research Consortium for the Participating Institutions. The Participating Institutions are the American Museum of Natural History, Astrophysical Institute Potsdam, University of Basel, University of Cambridge, Case Western Reserve University, University of Chicago, Drexel University, Fermilab, the Institute for Advanced Study, the Japan Participation Group, Johns Hopkins University, the Joint Institute for Nuclear Astrophysics, the Kavli Institute for Particle Astrophysics and Cosmology, the Korean Scientist Group, the Chinese Academy of Sciences (LAMOST), Los Alamos National Laboratory, the Max-Planck-Institute for Astronomy (MPIA), the Max-Planck-Institute for Astrophysics

(MPA), New Mexico State University, Ohio State University, University of Pittsburgh, University of Portsmouth, Princeton University, the United States Naval Observatory, and the University of Washington.

REFERENCES

Akritas M. G., Siebert J., 1996, MNRAS, 278, 919
Antonucci R. R. J., Ulvestad J. S., 1985, ApJ, 294, 158
Baum S. A., Heckman T. M., 1989, ApJ, 336, 702
Best P. N., Kauffmann G., Heckman T. M. et al., 2005, MNRAS, 362, 25
Best P. N., Kaiser C. R., Heckman T. M., Kauffmann G., 2006, MNRAS, 368, L67
Bicknell G. V., 1995, ApJS, 101, 29
Bîrzan L., Rafferty D. A., McNamara B. R., Wise M. W., Nulsen P. E. J., 2004, ApJ, 607, 800
Blandford R. D., Znajek R. L., 1977, MNRAS, 179, 433
Blandford R. D., Königl A., 1979, ApJ, 232, 34
Blandford R. D., Payne D. G., 1982, MNRAS, 199, 883
Bloom S. D., Marscher A. P., Moore E. M. et al., 1999, ApJS, 122, 1
Bower R. G., Benson A. J., Malbon R. et al., 2006, MNRAS, 370, 645
Brinkmann W., Yuan W., Siebert J., 1997, A&A, 319, 413
Brotherton M. S., 1996, ApJS, 102, 1
Browne I. W. A., Murphy D. W., 1987, MNRAS, 226, 601
Brunthaler A., Falcke H., Bower G. C. et al., 2000, A&A, 357, L45
Cao X. W., 2000, A&A, 355, 44
Cao X. W., Jiang D. R., 1999, MNRAS, 307, 802
Cao X. W., Jiang D. R., 2001, MNRAS, 320, 347
Cao X. W., 2003, ApJ, 599, 147
Celotti A., Fabian A. C., 1993, MNRAS, 264, 228
Celotti A., Padovani P., Ghisellini G., 1997, MNRAS, 286, 415 (C97)
Chen Z. Y., Gu M. F., Cao X., 2009, MNRAS, submitted
Comastri A., Fossati G., Ghisellini G., Molendi S., 1997, ApJ, 480, 534
Cooper N. J., Lister M. L., Kochanczyk M. D., 2007, ApJS, 171, 376
Corbett E. A., Robinson A., Axon D. J. et al., 1996, MNRAS, 281, 737
Croton D., Springel V., White S. D. M. et al., 2006, MNRAS, 365, 11
Donato D., Ghisellini G., Tagliaferri G., Fossati G., 2001, A&A, 375, 739
Donato D., Sambruna R. M., Gliozzi M., 2005, A&A, 433, 1163
Fabian A. C., Sanders J. S., Allen S. W. et al., 2003, MNRAS, 344, L43
Falcke H., Malkan M. A., Biermann P. L., 1995, A&A, 298, 375
Fan Z. H., Cao X., Gu M. F., 2006, ApJ, 646, 8
Fey A. L., Clegg A. W., Fomalont E. B., 1996, ApJS, 105, 299
Fey A. L., Charlot P., 1997, ApJS, 111, 95
Fey A. L., Charlot P., 2000, ApJS, 128, 17
Fossati G., Maraschi L., Celotti A., Comastri A., Ghisellini G., 1998, MNRAS, 299, 433
Francis P. J., Hewett P. C., Foltz C. B. et al., 1991, ApJ, 373, 465
Galbiati E., Caccianiga A., Maccacaro T. et al., 2005, A&A, 430, 927
Gallimore J. F., Axon D. J., O'Dea C. P., Baum S. A., Pedlar A., 2006, AJ, 132, 546
Gambill J. K., Sambruna R. M., Chartas G. et al., 2003, A&A, 401, 505
Gelfand J. D., Lazio T. J. W., Gaensler B. M., 2005, ApJS, 159, 242
Ghisellini G., Padovani P., Celotti A., Maraschi L., 1993, ApJ, 407, 65
Ghisellini G., Celotti A., Fossati G., Maraschi L., Comastri A., 1998, MNRAS, 301, 451
Güijosa A., Daly R. A., 1996, ApJ, 461, 600
Ho L. C., Filippenko A. V., Sargent W. L. W., Peng C. Y., 1997, ApJS, 112, 391
Hough D. H., Vermeulen R. C., Readhead A. C. S. et al., 2002, AJ, 123, 1258
Hutter D. J., Mufson S. L., 1986, ApJ, 301, 50
Imanishi M., Ueno S., 1999, ApJ, 527, 709
Isobe T., Feigelson E. D., Nelson P. I., 1986, ApJ, 306, 490
Isobe T., Feigelson E. D., Akritas M. G., Babu G. J., 1990, ApJ, 364, 104
Jackson N., Browne I. W. A., 1991, MNRAS, 250, 414

Jiang D. R., Cao X., Hong X., 1998, ApJ, 494, 139 (J98)
Jorstad S. G., Marscher A. P., Mattox J. R. et al., 2001, ApJS, 134, 181
Kaiser C. R., Dennett-Thorpe J., Alexander P., 1997, MNRAS, 292, 723
Kellermann K. I., Lister M. L., Homan D. C. et al., 2004, ApJ, 609, 539
Kharb P., Shastri P., 2004, A&A, 425, 825
Königl A., 1981, ApJ 243, 700
Kovalev Y. Y., Kellermann K. I., Lister M. L. et al., 2005, AJ, 130, 2473
Kuraszkiewicz J. K. et al., 2004, ApJS, 150, 165
Lähteenmäki A., Valtaoja E., 1999, ApJ, 521, 493
Lister M. L., 2001, ApJ, 562, 208
Liu Y., Jiang D. R., Gu M. F., 2006, ApJ, 637, 669
Macdonald D., Thorne K. S., 1982, MNRAS, 198, 345
Macklin J. T., 1982, MNRAS, 199, 1119
Maraschi L., Tavecchio F., 2003, ApJ, 593, 667 (MT03)
Marcha M. J. M., Browne I. W. A., Impey C. D., Smith P. S., 1996, MNRAS, 281, 425
Marscher A. P., 1987, in Superluminal Radio Sources, ed. J. A. Zensus & T. J. Pearson (Cambridge: Cambridge Univ. Press), 280
Marshall H. L., Schwartz D. A., Lovell J. E. J. et al., 2005, ApJS, 156, 13
McNamara B. R., Wise M., Nulsen P. E. J. et al., 2000, ApJ, 534, L135
Meier D., Koide S., Uchida Y., 2001, Science, 291, 84
Netzer H., 1990, in Active Galactic Nuclei, ed. R. D. Blandford, H. Netzer, & L. Woltjer (Berlin: Springer), 57
Nusser A., Silk J., Babul A., 2006, MNRAS, 373, 739
Pedlar A., Ghataure H. S., Davies R. D. et al., 1990, MNRAS, 246, 477
Perlman E. S., Stocke J. T., 1993, ApJ, 406, 430
Perlman E. S., Stocke J. T., Shaffer D. B., Carilli C. L., Ma C., 1994, ApJ, 424, L69
Punsly B., 1995, AJ, 109, 1555
Punsly B., Tingay S. J., 2005, ApJ, 633, L89
Rawlings S. G., Saunders R. D. E., Eales S. A., Mackay C. D., 1989, MNRAS, 240, 701
Rawlings S., Saunders R. 1991, Nature, 349, 138
Readhead A. C. S., 1994, ApJ, 426, 51
Rector T. A., Stocke J. T., 2001, AJ, 122, 565
Reich W., Fürst E., Reich P. et al., 2000, A&A, 363, 141
Rokaki E., Lawrence A., Economou F., Mastichiadis A., 2003, MNRAS, 340, 1298
Saikia D. J., Junor W., Cornwell T. J. et al., 1990, MNRAS, 245, 408
Saunders R., Baldwin J. E., Rawlings S., Warner P. J., Miller L., 1989, MNRAS, 238, 777
Scarpa R., Falomo R., 1997, A&A, 325, 109
Schmitt J. H. M. M., 1985, ApJ, 293, 178
Sergeev S. G., Pronik V. I., Sergeeva E. A., Malkov Y. F., 1999, AJ, 118, 2658
Shapley A., Fabbiano G., Eskridge P. B., 2001, ApJS, 137, 139
Siebert J., Brinkmann W., Drinkwater M. J. et al., 1998, MNRAS, 301, 261
Stanghellini C., Baum S. A., O'Dea C. P., Morris G. B., 1990, A&A, 233, 379
Tavecchio F., Maraschi L., Sambruna R. M. et al., 2006, ApJ, 641, 732
Thorne K. S., Blandford R. D., 1982, in Extragalactic Radio Sources, IAU Symp. 97, 255
Tinti S., Dallacasa D., de Zotti G., Celotti A., Stanghellini C., 2005, A&A, 432, 31
Ulvestad J., Johnston K., Perley R., Fomalont E., 1981, AJ, 86, 1010
Vermeulen R. C., Cohen M. H., 1994, ApJ, 430, 467
Walsh D., Carswell R. F., 1982, MNRAS, 200, 191
Wang T. G., Lu Y. J., Zhou Y. Y., 1998, ApJ, 493, 1
Wang J. M., Luo B., Ho L. C., 2004, ApJ, 615, L9
Wardle J. F. C., Homan D. C., Ojha R., Roberts D. H., 1998, Nature, 395, 457
Wilkes B. J., 1986, MNRAS, 218, 331
Wills B. J., Browne I. W. A., 1986, ApJ, 302, 56
Worrall D. M., Birkinshaw M., 2006, Lecture Notes Phys., 693, 39
Wu Z. Z., Jiang D. R., Gu M. F., Liu Y., 2007, A&A, 466, 63
Zhang J. S., Fan J. H., 2003, Chinese J. Astron. Astrophys., 3, 415

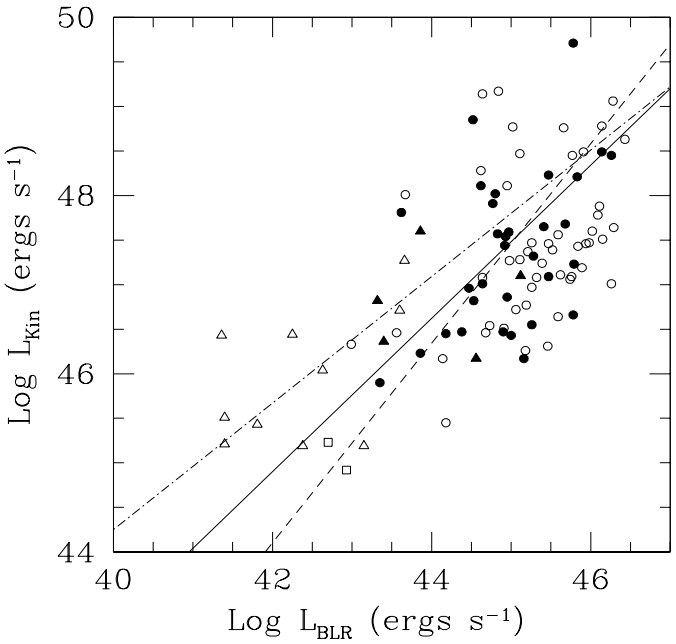

Figure 1. The bulk kinetic power versus BLR luminosity. The circles represent quasars, and the triangles are BL Lac objects, while the rectangles show radio galaxies. The filled symbols are the sources in the redshift range $0.5 < z < 1.0$. The solid line is the fitted line for the whole sample using the OLS bisector method, and the dashed line is fitted for quasars only, while the dot-dashed line is fitted for BL Lac objects only.

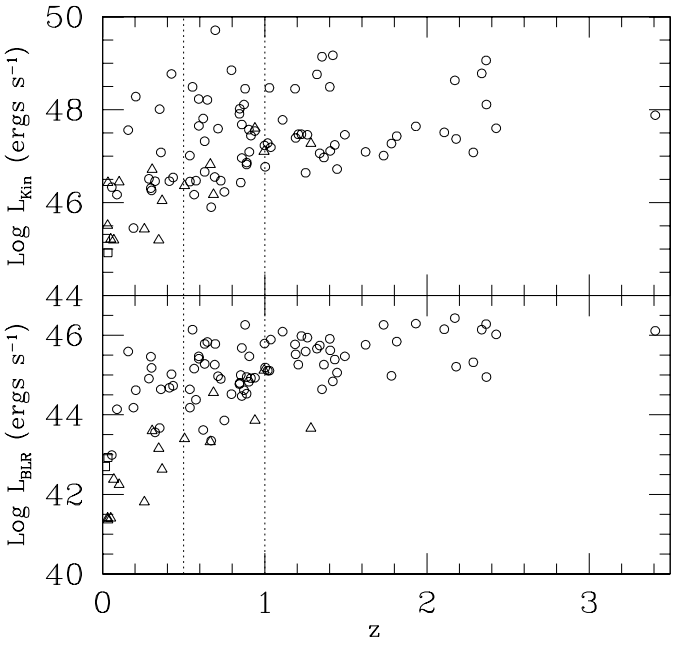

Figure 2. The bulk kinetic power versus redshift (upper panel) and the BLR luminosity versus redshift planes (lower panel) for the sample. The circles represent quasars, and the triangles are BL Lac objects, while the rectangles show radio galaxies. The restricted redshift range, $0.5 < z < 1.0$, is indicated with the dotted lines.

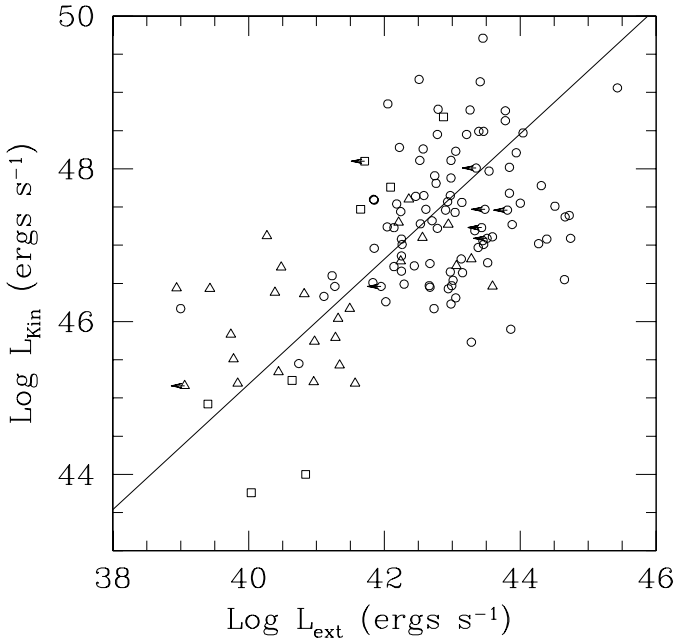

Figure 3. The bulk kinetic power versus radio 5 GHz extended luminosity. The symbols are the same as in Fig. 2. The arrows indicate the upper limit of extended luminosity. The solid line is the bisector linear fit using Schmitt-binning method for censored data (see text for details).

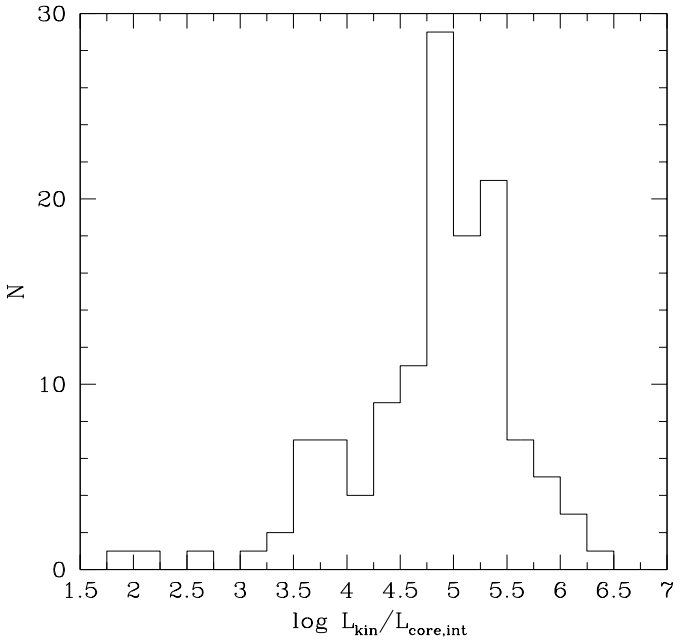

Figure 4. The histogram shows the distribution of the ratio of the bulk kinetic power to intrinsic core radio radiative luminosities.

Table 1. VLBI and X-ray Data of the Sample.

Source	Type	z	$\nu_{\rm s}$ (GHz)	$f_{\rm c}$ (Jy)	$\theta_{\rm d}$ (mas)	Refs.	$\mu_{\rm app}$ (mas yr^{-1})	Refs.	$f_{\rm 1keV}$ (μJy)	Refs.
0003−066	BL	0.347	15.0	1.850	0.17	1	0.010	11	0.169	13
0007+106	Qc	0.089	43.0	1.540	0.07	2	0.237	2	2.740	14
0016+731	Qc	1.781	15.0	1.020	0.10	1	0.220	4	0.050	15
0035+413	Qc	1.353	15.0	0.380	0.27	1	0.100	11	0.099	14
0106+013	Qc	2.107	15.0	2.320	0.12	1	0.280	11	0.220	4
0108+388	G	0.670	8.5	0.240	0.21	3	0.100	12	0.060	16
0112−017	Qc	1.365	15.0	0.480	0.08	1	0.020	11	0.150	15
0133+207	Ql	0.425	10.7	0.082	0.22	4	0.240	4	0.753	4
0133+476	Qc	0.859	15.0	4.710	0.09	1	0.040	11	0.300	15
0153+744	Qc	2.338	15.0	0.190	0.11	1	0.080	4	1.000	4
0202+149	Qc	0.405	15.0	1.760	0.16	1	0.250	11	0.060	15
0208−512	Qc	1.003	5.0	2.770	0.35	4	0.600	4	0.080	4
0212+735	Qc	2.367	15.0	2.400	0.20	1	0.090	4	0.260	15
0219+428	BL	0.444	43.2	0.593	0.02	5	1.110	5	1.560	15
0234+285	Qc	1.207	22.3	1.700	0.10	4	0.300	4	0.150	4
0235+164	BL	0.940	5.0	1.750	0.50	4	0.840	4	0.170	4
0316+413	G	0.017	22.2	6.000	0.30	4	0.540	4	18.000	4
0333+321	Qc	1.263	15.0	1.840	0.12	1	0.400	11	0.440	15
0336−019	Qc	0.852	15.0	1.780	0.07	1	0.420	5	0.100	17
0415+379	G	0.049	86.2	2.900	0.13	4	1.540	4	3.283	4
0420−014	Qc	0.915	43.2	2.724	0.06	5	0.290	11	0.370	15
0430+052	G	0.033	15.0	1.710	0.10	1	2.660	4	10.000	4
0440−003	Qc	0.844	15.0	0.620	0.15	1	0.340	5	0.189	13
0454+844	BL	0.112	5.0	1.300	0.55	4	0.140	4	0.050	4
0458−020	Qc	2.286	43.2	0.934	0.02	5	0.150	4	0.100	17
0528+134	Qc	2.060	43.2	3.875	0.07	5	0.400	4	0.310	15
0552+398	Qp	2.365	8.4	2.620	0.73	6	0.040	12	0.490	6
0605−085	Qc	0.872	15.0	1.790	0.27	1	0.180	11	0.168	18
0607−157	Qc	0.324	15.0	6.920	0.19	1	0.170	11	0.290	14
0615+820	Qc	0.710	5.0	0.610	0.50	4	0.050	4	0.040	15
0642+449	Qp	3.408	15.0	2.920	0.12	1	0.010	11	0.120	15
0710+439	G	0.518	5.0	0.630	0.96	4	0.040	4	0.550	4
0716+714	BL	0.300	43.2	0.390	0.04	5	1.200	5	0.990	15
0723+679	Ql	0.846	43.0	0.677	0.06	7	0.190	12	0.162	18
0735+178	BL	0.424	15.0	0.950	0.14	1	0.640	11	0.220	15
0736+017	Qc	0.191	15.0	1.450	0.06	1	0.930	11	0.640	15
0738+313	Qc	0.630	15.0	0.870	0.11	1	0.070	11	0.075	14
0745+241	Qc	0.409	15.0	0.830	0.10	1	0.320	11	0.131	19
0748+126	Qc	0.889	15.0	2.860	0.11	1	0.274	11	0.209	20
0754+100	BL	0.266	15.0	1.420	0.11	1	0.700	11	0.720	15
0804+499	Qc	1.432	15.0	1.020	0.09	1	0.130	11	0.170	15
0808+019	BL	0.930	15.0	1.270	0.04	1	0.110	11	0.380	15
0814+425	BL	0.258	15.0	1.080	0.06	1	0.320	11	0.050	15
0823+033	BL	0.506	15.0	1.100	0.07	1	0.480	11	0.415	13
0827+243	Qc	0.939	43.2	1.406	0.05	5	0.480	5	0.340	17
0829+046	BL	0.180	22.2	0.796	0.05	5	1.400	5	0.400	15
0836+710	Qc	2.172	43.2	1.570	0.06	5	0.240	5	2.260	15
0850+581	Qc	1.322	15.0	0.070	0.08	1	0.200	11	0.970	4
0851+202	BL	0.306	43.2	1.640	0.04	5	0.670	5	2.240	15
0859−140	Ql	1.339	15.0	1.170	0.09	1	0.260	11	0.171	14
0906+015	Qc	1.018	15.0	2.360	0.15	1	0.220	11	0.141	14
0906+430	Qc	0.670	5.0	0.875	0.10	4	0.180	4	0.090	4
0917+449	Qc	2.180	22.2	1.042	0.05	5	0.150	5	0.470	15
0917+624	Q	1.446	8.4	1.220	0.11	4	0.230	4	0.120	4
0923+392	Qc	0.695	15.0	0.230	0.34	1	0.180	4	0.370	4
0945+408	Qc	1.252	15.0	0.990	0.06	1	0.370	11	0.110	15
0953+254	Qc	0.712	15.0	0.360	0.12	1	0.310	11	0.097	14
0954+658	BL	0.368	5.0	0.477	0.19	4	0.440	4	0.160	15
1012+232	Qc	0.565	15.0	1.080	0.07	1	0.270	11	0.088	14
1015+359	Qc	1.226	15.0	0.710	0.13	1	0.200	11	0.051	14
1039+811	Qc	1.260	8.5	0.450	0.09	8	0.070	12	0.180	15

Table 1. *Continued.*

Source	Type	z	$\nu_{\rm s}$ (GHz)	$f_{\rm c}$ (Jy)	$\theta_{\rm d}$ (mas)	Refs.	$\mu_{\rm app}$ (mas yr^{-1})	Refs.	$f_{\rm 1keV}$ (μJy)	Refs.
1040+123	Qc	1.029	10.7	0.590	0.33	4	0.110	4	0.121	4
1049+215	Qc	1.300	15.0	1.220	0.16	1	0.140	11	0.064	14
1055+018	Qc	0.888	15.0	4.930	0.06	1	0.040	11	0.210	15
1055+201	Qc	1.110	15.0	0.260	0.10	1	0.180	11	0.164	20
1101+384	BL	0.031	15.0	0.450	0.10	1	1.330	4	36.100	15
1127−145	Qc	1.187	22.2	1.060	0.14	5	0.520	5	0.340	15
1128+385	Qc	1.733	15.0	0.940	0.05	1	0.010	11	0.061	14
1137+660	Ql	0.646	8.4	0.119	0.23	9	0.060	12	0.343	14
1150+812	Qc	1.250	5.0	0.460	0.50	4	0.110	4	0.200	4
1156+295	Qc	0.729	22.2	1.372	0.05	5	0.540	5	0.440	15
1219+285	BL	0.102	22.2	0.263	0.09	5	0.600	5	0.400	15
1222+216	Ql	0.435	22.2	0.960	0.06	5	0.900	5	0.410	17
1226+023	Qc	0.158	43.2	8.040	0.13	5	1.600	5	20.420	15
1228+127	G	0.004	15.0	1.390	0.33	1	3.070	4	0.680	4
1253−055	Qc	0.538	43.2	13.773	0.07	5	0.310	5	1.500	15
1302−102	Qc	0.286	15.0	0.530	0.09	1	0.310	11	0.723	14
1308+326	BL	0.996	15.0	2.590	0.14	1	0.750	4	0.110	15
1334−127	Qc	0.539	15.0	7.400	0.04	1	0.050	11	0.450	15
1345+125	G	0.121	8.5	0.480	0.89	10	0.160	11	0.038	21
1406−076	Q	1.494	22.2	0.833	0.07	5	0.630	5	0.075	14
1413+135	BL	0.247	15.0	1.420	0.04	1	0.450	11	0.050	15
1458+718	Qc	0.905	8.5	0.880	0.17	3	0.250	12	0.226	14
1508−055	Ql	1.191	15.0	0.590	0.09	1	0.530	11	0.147	13
1510−089	Qc	0.360	43.2	1.458	0.05	5	0.850	11	0.490	15
1532+016	Qc	1.420	15.0	0.320	0.23	1	0.210	11	0.130	22
1546+027	Qc	0.412	15.0	2.760	0.08	1	0.050	11	0.840	15
1548+056	Qc	1.422	15.0	0.880	0.11	1	0.052	11	0.018	13
1606+106	Qc	1.226	15.0	1.850	0.17	1	0.500	11	0.080	17
1611+343	Qc	1.401	43.2	1.460	0.08	5	0.570	5	0.240	15
1618+177	Ql	0.555	10.7	0.086	0.20	4	0.100	4	0.300	4
1622−297	Q	0.815	43.2	2.355	0.06	5	0.400	5	0.080	17
1633+382	Qc	1.814	22.2	1.553	0.07	5	0.200	5	0.250	15
1637+826	G	0.023	10.7	0.670	0.20	4	0.300	4	0.300	4
1641+399	Qc	0.593	22.0	6.900	0.30	4	0.490	11	0.660	4
1642+690	Qc	0.751	15.0	1.180	0.05	1	0.380	11	0.145	18
1652+398	BL	0.034	15.0	0.540	0.21	1	0.960	5	10.100	17
1655+077	Qc	0.621	15.0	1.590	0.23	1	0.430	11	0.153	19
1656+053	Qc	0.879	15.0	0.660	0.23	1	0.090	11	0.353	14
1656+477	Qc	1.622	15.0	0.680	0.09	1	0.060	11	0.041	14
1721+343	Ql	0.205	10.7	0.109	0.24	4	0.280	4	1.900	4
1730−130	Qc	0.902	43.2	5.850	0.07	5	0.480	11	0.630	17
1749+096	BL	0.320	15.0	5.550	0.05	1	0.150	11	0.150	15
1749+701	BL	0.770	15.0	0.570	0.08	1	0.260	4	0.150	15
1758+388	Qp	2.092	15.0	1.620	0.13	1	0.002	11	0.131	14
1800+440	Qc	0.663	15.0	1.380	0.03	1	0.560	11	0.111	14
1803+784	BL	0.684	5.0	1.436	0.20	4	0.004	4	0.160	4
1807+698	BL	0.051	15.0	0.830	0.12	1	2.600	4	0.300	15
1823+568	BL	0.664	15.0	2.140	0.12	1	0.120	4	0.200	4
1828+487	Ql	0.692	15.0	1.300	0.07	1	0.380	11	0.344	19
1830+285	Ql	0.594	8.5	0.380	0.24	8	0.130	12	0.310	6
1845+797	Qc	0.057	15.0	0.300	0.13	1	0.600	11	5.470	15
1921−293	Qc	0.352	15.0	0.410	0.19	1	0.190	11	1.060	15
1928+738	Qc	0.302	15.0	2.580	0.11	1	0.600	4	0.550	4
2007+776	BL	0.342	5.0	1.361	0.19	4	0.180	4	0.110	4
2131−021	BL	1.285	15.0	1.150	0.13	1	0.120	11	0.050	15
2134+004	Qp	1.932	15.0	2.020	0.15	1	0.020	11	0.260	15
2136+141	Qc	2.427	15.0	2.040	0.12	1	0.020	11	0.120	23
2144+092	Qc	1.113	15.0	0.550	0.07	1	0.030	11	0.035	13
2145+067	Qc	0.999	15.0	7.970	0.11	1	0.030	11	0.360	16
2200+420	BL	0.069	15.0	2.960	0.10	1	1.410	11	2.200	15
2201+315	Qc	0.298	15.0	2.710	0.08	1	0.340	11	3.780	23
2223−052	Qc	1.404	15.0	1.980	0.10	4	0.490	11	0.270	15

Table 1. *Continued.*

Source	Type	z	$\nu_{\rm s}$ (GHz)	$f_{\rm c}$ (Jy)	$\theta_{\rm d}$ (mas)	Refs.	$\mu_{\rm app}$ (mas yr^{-1})	Refs.	$f_{\rm 1keV}$ (μJy)	Refs.
2230+114	Qc	1.037	43.2	2.428	0.04	5	0.500	4	0.730	15
2234+282	Qc	0.795	15.0	0.460	0.32	1	0.120	11	0.050	16
2243−123	Qc	0.630	15.0	1.920	0.17	1	0.290	11	0.279	24
2251+158	Qc	0.859	43.2	2.015	0.05	5	0.530	5	1.370	15
2345−167	Qc	0.576	15.0	1.460	0.10	1	0.030	11	0.180	16

Column (1): IAU name; Column (2): classification of the source (Q= quasars; Qc= core-dominated quasars; Ql= lobe-dominated quasars; Qp= GHz peaked quasars; BL= BL Lac objects; G= radio galaxies); Column (3): redshift z; Column (4): observation frequency $\nu_{\rm s}$ in GHz; Column (5): core radio flux density $f_{\rm c}$ at frequency $\nu_{\rm s}$; Column (6): VLBI core size $\theta_{\rm d}$ in mas; Column (7): reference for the VLBI data; Column (8): the proper motion $\mu_{\rm app}$; Column (9): reference for the proper motion; Column (10): 1 keV X-ray flux density $f_{\rm 1keV}$ in μJy; Column (11): reference for the X-ray flux.

References: (1) Kovalev et al. (2005); (2) Brunthaler et al. (2000); (3) Fey & Charlot (1997); (4) J98; (5) Jorstad et al. (2001); (6) Rokaki et al. (2003); (7) Lister (2001); (8) Fey & Charlot (2000); (9) Hough et al. (2002); (10) Fey, Clegg & Fomalont (1996); (11) Kellermann et al. (2004); (12) Vermeulen & Cohen (1994); (13) Siebert et al. (1998); (14) Brinkmann, Yuan & Siebert (1997); (15) Donato et al. (2001); (16) Ghisellini et al. (1993); (17) Comastri et al. (1997); (18) Gambill et al. (2003); (19) Marshall et al. (2005); (20) Reich et al. (2000); (21) Imanishi & Ueno (1999); (22) Galbiati et al. (2005); (23) Bloom et al. (1999); (24) Donato, Sambruna & Gliozzi (2005).

Table 2. Derived Jet Parameters and Luminosity of the Sample.

Source	θ (degree)	Γ	δ	n_1 (cm^{-3})	log L_{kin} (erg s^{-1})	log L_{BLR} (erg s^{-1})	Refs.	log $L_{ext,5GHz}$ (erg s^{-1})	Refs.
0003−066	56.7	1.0	1.1	9.48E+04	45.19	43.15	1	41.57	21
0007+106	51.0	1.9	1.1	1.32E+04	46.17	44.14	2	39.00	22
0016+731	4.4	17.7	12.4	6.75E+04	47.27	44.98	1	43.88	23
0035+413	17.1	19.2	1.1	5.01E+06	49.14	44.64	1	43.41	24
0106+013	2.8	23.9	20.1	1.15E+05	47.51	46.15	1	44.51	25
0108+388	25.7	5.9	1.5	1.24E+05	47.47	...	...	41.65	26
0112−017	23.4	1.7	2.3	9.52E+04	46.97	45.26	1	43.38	25
0133+207	18.0	28.6	0.7	2.09E+06	48.77	45.02	1	43.26	25
0133+476	4.5	3.7	6.7	4.42E+04	46.96	44.47	1	41.85	21
0153+744	14.5	12.3	2.3	2.23E+06	48.78	46.14	1	42.79	23
0202+149	12.1	6.6	4.5	1.63E+04	46.60	...	...	41.23	21
0208−512	2.2	32.0	25.9	2.07E+04	46.77	45.19	3	43.52^b	27
0212+735	8.9	8.4	6.2	5.06E+05	48.11	44.95	1	42.52	25
0219+428	3.1	38.0	14.6	1.89E+04	46.73	...	...	43.06	28
0234+285	4.8	20.6	10.5	1.05E+05	47.47	45.26	1	42.61	25
0235+164	2.4	66.5	14.9	1.37E+05	47.60	43.86	1	42.36	25
0316+413	88.9	1.3	0.8	4.76E+03	45.23	42.70	4	40.64	29
0333+321	3.3	27.5	15.4	1.01E+05	47.46	45.94	5	42.90	5
0336−019	2.5	19.7	22.5	9.73E+03	46.43	45.00	1	42.94	25
0415+379	21.9	17.3	0.8	2.09E+05	47.76	...	...	42.09	23
0420−014	5.7	15.6	9.2	1.01E+05	47.44	44.92	1	42.24	25
0430+052	8.6	6.0	6.6	3.43E+02	44.92	42.93	6	39.40	22
0440−003	6.7	29.0	4.6	2.89E+05	47.91	44.77	1	42.74	25
0454+844	49.0	1.4	1.3	3.45E+03	45.34	...	...	40.44	30
0458−020	3.1	13.8	17.7	4.42E+04	47.08	45.32	1	44.39	25
0528+134	2.6	38.7	19.0	3.22E+05	47.97	...	...	43.54	21
0552+398	25.9	4.9	1.7	5.03E+06	49.06	46.28	7	45.43	7,31
0605−085	11.9	13.4	3.1	4.77E+05	48.11	44.62	1	42.98	25
0607−157	9.9	3.9	5.4	1.39E+04	46.46	43.56	1	<41.95	25
0615+820	40.0	2.6	1.3	1.02E+05	47.22	...	...	42.78	23
0642+449	7.8	2.2	3.9	5.30E+05	47.88	46.11	1	42.98	25
0710+439	74.8	3.5	0.4	2.40E+06	48.68	...	...	42.87	26
0716+714	4.8	49.5	5.5	6.91E+04	47.30	...	...	42.21	21
0723+679	11.9	15.3	2.8	3.82E+05	48.02	44.80	1	43.84	25
0735+178	6.1	25.2	6.2	4.70E+04	47.12	...	...	40.27	30
0736+017	3.3	12.3	16.5	1.05E+03	45.45	44.18	1	40.74	25
0738+313	20.8	2.7	2.8	2.64E+04	46.66	45.78	1	42.25	25
0745+241	9.6	8.6	5.6	1.20E+04	46.49	...	...	42.29	30
0748+126	4.0	13.2	14.3	2.69E+04	46.86	44.95	5	42.25	5
0754+100	6.6	12.8	8.1	8.83E+03	46.38	...	...	40.39	30
0804+499	6.9	8.8	8.3	6.67E+04	47.24	45.39	1	42.04	25
0808+019	1.9	9.6	17.3	1.11E+04	46.46	...	...	43.59	30
0814+425	5.4	6.2	9.2	1.11E+03	45.43	41.81	1	41.34	25
0823+033	4.2	14.6	13.7	8.33E+03	46.36	43.40	1	40.82	25
0827+243	4.0	32.1	10.7	1.23E+05	47.54	44.93	8	42.18	32
0829+046	4.8	17.6	11.3	1.97E+03	45.74	...	...	40.97	30
0836+710	4.8	29.3	8.5	1.50E+06	48.63	46.43	1	43.78	25
0850+581	8.7	37.6	2.2	2.02E+06	48.76	45.66	1	43.78	25
0851+202	6.3	14.3	8.3	1.87E+04	46.71	43.60	1	40.48	25
0859−140	3.9	16.8	14.7	4.13E+04	47.06	45.74	1	43.45	25
0906+015	6.3	12.2	8.7	7.05E+04	47.28	45.11	1	42.53	25
0906+430	1.8	11.0	19.5	2.95E+03	45.90	43.35	1	43.86	25
0917+449	3.7	13.1	15.2	8.70E+04	47.37	45.21^a	9	44.66	33
0917+624	2.5	16.5	21.8	1.91E+04	46.72	45.06	1	42.14	25
0923+392	15.9	43.4	0.6	1.77E+07	49.71	45.78	1	43.45	25
0945+408	2.4	22.7	23.8	1.55E+04	46.64	45.59	1	43.15	25
0953+254	8.4	22.4	3.8	1.39E+05	47.59	44.97	1	41.85	25
0954+658	6.8	10.3	8.3	4.17E+03	46.04	42.63	1	41.32	25
1012+232	4.9	9.3	11.3	5.70E+03	46.17	45.16	10	42.73	34
1015+359	7.6	15.2	6.1	1.07E+05	47.47	45.98	9	<43.48	35
1039+811	7.4	4.9	7.0	2.53E+04	46.76	...	...	42.67	23

Table 2. *Continued.*

Source	θ (degree)	Γ	δ	n_1 (cm^{-3})	log $L_{\rm kin}$ (erg s^{-1})	log $L_{\rm BLR}$ (erg s^{-1})	Refs.	log $L_{\rm ext,5GHz}$ (erg s^{-1})	Refs.
1040+123	18.0	11.8	1.6	1.10E+06	48.47	45.11	1	44.04	25
1049+215	9.5	10.0	5.3	1.35E+05	47.55	...	...	44.00	36
1055+018	1.9	5.5	10.7	2.80E+04	46.82	44.53	1	43.13	25
1055+201	10.0	15.9	3.7	2.19E+05	47.78	46.09	11	44.31	30
1101+384	29.3	3.3	1.8	1.67E+03	45.51	41.40	12	39.78	28
1127−145	3.5	69.7	7.2	9.81E+05	48.45	45.77	1	43.21	25
1128+385	6.6	2.1	3.7	7.96E+04	47.01	46.26	9	42.26	30
1137+660	45.7	5.1	0.6	6.98E+05	48.21	45.83	1	43.94	25
1150+812	15.1	11.2	2.3	6.81E+05	48.26	...	...	42.57	30
1156+295	2.5	22.2	23.1	1.05E+04	46.47	44.90	5	42.99	5
1219+285	25.1	7.0	1.4	1.12E+04	46.44	42.25	13	38.94	28
1222+216	3.6	27.4	13.9	1.21E+04	46.54	44.73	14	43.01	21
1226+023	6.2	27.3	5.6	1.29E+05	47.56	45.59	1	43.14	25
1228+127	85.3	1.6	0.7	1.21E+02	44.00	...	...	40.84	23
1253−055	4.1	10.4	13.5	3.83E+04	47.01	44.64	1	43.46	25
1302−102	14.3	6.3	3.7	1.33E+04	46.51	44.91	1	41.83	25
1308+326	2.2	45.3	22.5	4.41E+04	47.10	45.12	1	42.56	25
1334−127	0.5	9.8	19.4	1.06E+04	46.45	44.18	1	42.67	25
1345+125	75.3	6.4	0.2	5.13E+05	48.10	...	...	<41.71	35
1406−076	2.2	61.1	18.1	1.01E+05	47.46	45.47	15	<43.81	33
1413+135	2.1	10.7	18.6	5.48E+02	45.16	...	...	<39.06	37
1458+718	6.4	13.1	8.3	4.58E+04	47.09	45.47	1	44.74	25
1508−055	3.1	43.6	13.4	8.48E+04	47.39	45.52	15	44.72	36
1510−089	5.2	27.9	7.5	4.26E+04	47.08	44.64	1	42.25	25
1532+016	8.0	49.7	2.0	5.15E+06	49.17	44.84	1	42.51	25
1546+027	7.7	2.4	4.2	1.85E+04	46.46	44.68	1	41.27	25
1548+056	14.3	3.6	4.0	5.14E+04	47.02	...	...	44.27	36
1606+106	3.2	42.8	12.5	1.57E+05	47.65	...	...	42.58	30
1611+343	2.9	82.9	9.1	1.07E+06	48.49	45.91	1	43.39	25
1618+177	33.1	10.3	0.6	1.17E+06	48.49	46.14	5	43.46	5
1622−297	4.9	21.3	9.8	6.06E+04	47.23	...	...	<43.43	35
1633+382	4.2	15.7	13.7	9.90E+04	47.43	45.84	1	43.04	25
1637+826	77.7	1.1	1.0	4.94E+02	43.76	...	...	40.04	23
1641+399	6.1	29.5	5.4	5.91E+05	48.23	45.47	1	43.05	25
1642+690	2.5	16.7	21.7	6.14E+03	46.23	43.86	1	42.98	25
1652+398	45.0	4.2	0.8	1.24E+04	46.43	41.36	12	39.43	28
1655+077	6.8	27.7	4.7	2.28E+05	47.81	43.62	5	42.76	5
1656+053	24.2	7.9	1.3	1.12E+06	48.45	46.26	5	42.78	5
1656+477	11.1	4.5	5.1	5.54E+04	47.09	45.76	16	<43.51	33
1721+343	29.7	14.5	0.5	7.05E+05	48.28	44.62	1	42.22	25
1730−130	3.6	26.2	14.1	1.32E+05	47.57	44.83	17	42.93	32
1749+096	1.1	8.9	17.3	2.62E+03	45.83	...	...	39.74	28
1749+701	6.8	11.8	8.0	2.29E+04	46.79	...	...	42.24	38
1758+388	24.2	1.0	1.3	1.43E+06	46.73	...	...	42.44	39
1800+440	0.9	28.2	46.7	1.91E+03	45.73	...	...	43.28	36
1803+784	10.6	1.1	1.6	1.04E+05	46.17	44.56	1	41.49	25
1807+698	9.8	10.5	5.0	6.15E+02	45.21	41.40	12	40.96	28
1823+568	10.4	4.7	5.5	2.95E+04	46.82	43.32	1	43.28	25
1828+487	3.8	15.0	15.2	1.30E+04	46.55	45.26	1	44.65	25
1830+285	22.0	6.9	1.8	1.79E+05	47.65	45.41	1	42.97	25
1845+797	41.9	3.8	0.9	1.02E+04	46.33	42.99	5	41.11	5
1921−293	25.5	9.0	1.1	3.90E+05	48.01	43.67	18	<43.35	32
1928+738	5.3	11.5	10.8	6.88E+03	46.26	45.18	1	42.02	25
2007+776	5.2	5.1	8.4	2.66E+03	45.79	...	...	41.28	28
2131−021	9.5	7.8	5.8	7.38E+04	47.27	43.66	19	42.94	32
2134+004	18.2	2.1	2.9	3.41E+05	47.64	46.29	1	42.46	25
2136+141	10.6	2.6	4.1	2.44E+05	47.60	46.02	1	41.84	25
2144+092	17.4	2.1	3.0	3.30E+04	46.65	...	...	42.97	30
2145+067	3.9	3.6	6.6	8.31E+04	47.23	45.79	1	42.14	25
2200+420	5.8	7.0	9.3	6.27E+02	45.19	42.38	20	39.84	28
2201+315	5.2	7.1	10.0	8.23E+03	46.31	45.46	1	43.05	25
2223−052	2.1	33.1	26.4	4.53E+04	47.11	45.62	1	43.59	25

Table 2. *Continued.*

Source	θ (degree)	Γ	δ	n_1 (cm^{-3})	log L_{kin} (erg s^{-1})	log L_{BLR} (erg s^{-1})	Refs.	log $L_{ext,5GHz}$ (erg s^{-1})	Refs.
2230+114	2.7	27.9	20.3	5.51E+04	47.19	45.89	1	43.33	25
2234+282	20.9	16.8	0.9	2.58E+06	48.85	44.52	1	42.05	25
2243−123	8.4	12.6	5.8	7.80E+04	47.32	45.28	1	42.70	25
2251+158	3.8	32.4	11.5	1.67E+05	47.68	45.68	1	43.84	25
2345−167	20.7	1.6	2.3	3.55E+04	46.47	44.38	5	42.66	25

Column (1): IAU name; Column (2): the viewing angle of jet θ; Column (3): the Lorentz factor Γ; Column (4): the Doppler factor δ; Column (5): the normalization factor of electron energy distribution n_1; Column (6): the bulk kinetic power of jet L_{kin}; Column (7): the total luminosity in broad emission lines L_{BLR}, ^{a}: also see Chen, Gu & Cao (2009); Column (8): the references for flux of broad emission lines used to estimate L_{BLR}; Column (9): the radio extended 5 GHz luminosity $L_{ext,5GHz}$, ^{b}: from ATCA images; Column (10): the references for the radio extended flux.

References: (1) Cao & Jiang (1999); (2) Sergeev et al. (1999); (3) Scarpa & Falomo (1997); (4) Ho et al. (1997); (5) Liu, Jiang & Gu (2006); (6) Wang, Lu & Zhou (1998); (7) Rokaki et al. (2003); (8) Our unpublished measurements of Mg II line; (9) SDSS spectra; (10) Brotherton (1996); (11) Kuraszkiewicz et al. (2004); (12) C97; (13) Marcha et al. (1996); (14) Fan, Cao & Gu (2006); (15) Wilkes (1986); (16) Walsh & Carswell (1982); (17) Cao (2000); (18) Jackson & Browne (1991); (19) Rector & Stocke (2001); (20) Corbett et al. (1996); (21) Cooper, Lister & Kochanczyk (2007); (22) Wills & Browne (1986); (23) Kharb & Shastri (2004); (24) Gelfand et al. (2005); (25) Cao & Jiang (2001); (26) Vermeulen & Cohen (1994); (27) Marshall et al. (2005); (28) Perlman & Stocke (1993); (29) Pedlar et al. (1990); (30) Antonucci & Ulvestad (1985); (31) Stanghellini et al. (1990); (32) Browne & Murphy (1987); (33) Punsly (1995); (34) Saikia et al. (1990); (35) Ulvestad et al. (1981); (36) Zhang & Fan (2003); (37) Perlman et al. (1994); (38) Wu et al. (2007); (39) Tinti et al. (2005).